



Detection of fishing pressure using ecological network indicators derived from ecosystem models

Maysa Ito^{a,b,*}, Ghassen Halouani^a, Pierre Cresson^a, Carolina Giraldo^a, Raphaël Girardin^a

^a Ifremer, Channel and North Sea Fisheries Research Unit, HMMN, F-62200 Boulogne-sur-mer, France

^b Division of Marine Ecology, Marine Evolutionary Ecology, GEOMAR Helmholtz Centre for Ocean Research Kiel, Düsternbrooker Weg 20, 24105 Kiel, Germany

ARTICLE INFO

Keywords:

OSMOSE
Atlantis
Ecological network analysis
Network indicators
Fishery
Ecosystem model
English Channel

ABSTRACT

Marine ecosystems are exposed to multiple stressors, mainly fisheries that, whenever mismanaged, may cause irreversible damages to whole food webs. Ecosystem models have been applied to forecast fisheries impact on fish stocks and marine food webs. These impacts have been studied through the use of multiple indicators that help to understand ecosystem responses to stressors. This study focused on a category of ecological indicators derived from the network theory to quantify energy flows inside the food web. These indicators were computed using two ecosystem models applied to the Eastern English Channel (i.e. Atlantis and OSMOSE). This work aimed at investigating how several ecological network indicators respond to different levels of fishing pressure and evaluating their robustness to model structure and fishing strategies. We applied a gradient of fishing mortality using two ecosystem models and carried out ecological network analysis to obtain network-derived indicators. The results revealed that the indicators response is highly driven by the food web structure, although the model assumptions buffered some results. The indicators computed from OSMOSE outputs were more sensitive to changes in fishing pressure than those from Atlantis. However, once the food web from Atlantis was simplified to mimic the structure of OSMOSE model, the indicators of the modified Atlantis became more sensitive to the intensity of fishing pressure. The indicators related to amount of energy flow and to the organization of the flows in the food web were sensitive to the increase of fishing mortality for all fishing strategies. These indicators suggested that increasing fishing mortality jeopardizes the amount of energy mobilized by the food webs and simplifies the ecological interactions, which has implications for the resilience of marine ecosystems. The study shed light on the trophic networks structure and functioning of the ecosystems whenever exposed to disturbances. Furthermore, these indicators might be adequate for whole ecosystem assessments of health and contribute to ecosystem management.

1. Introduction

Healthy marine ecosystems are able to maintain proper ecological processes, providing essential services to humans. Currently, marine ecosystems are exposed to multiple stressors that are able to reshuffle species diversity (Magurran, 2016; Halpern et al., 2008) leading to changes in the ecosystem functioning, which generates uncertainties and jeopardizes the capacities to manage them properly (Ingeman et al., 2019). The stress caused to marine ecosystems was one of the motivations for the implementation of the European Marine Strategy Framework Directive (EU MSFD - DIRECTIVE 2008/56/EC) in 2008. The EU MSFD aims at developing strategies for protection, conservation and restoration of marine ecosystems using ecosystem-based approach to

management that ensures good environmental status (GES).

Environmental management has evolved from focusing on single-species to whole ecosystem (Garcia and Cochrane, 2005). In order to acquire a holistic perspective, it is necessary to advance the knowledge on ecosystem models, since they are able to depict not only complex ecological interactions but also connect them to socio-economic systems (Plagányi et al., 2011). Many ecosystem model frameworks exist and some are still in development, instead of choosing only one of them, a multi-model approach can be beneficial. This approach provides us with information about several aspects of the ecosystems that a single model would not suffice (Spence et al., 2018). The use of multiple models enables the comparison of the outputs, as well as the derived ecological indicators, which may confirm that the results are depicting ecosystem

* Corresponding author at: Ifremer, Channel and North Sea Fisheries Research Unit, HMMN, F-62200 Boulogne-sur-mer, France.

E-mail address: mito@geomar.de (M. Ito).

<https://doi.org/10.1016/j.ecolind.2023.110011>

Received 30 September 2022; Received in revised form 7 February 2023; Accepted 9 February 2023

Available online 15 February 2023

1470-160X/© 2023 The Authors. Published by Elsevier Ltd. This is an open access article under the CC BY license (<http://creativecommons.org/licenses/by/4.0/>).

responses (Shin et al., 2018), reducing the uncertainties arising from models assumptions (Smith et al., 2015). Such an approach is useful for risk assessment and informs more effectively strategies for adaptive management of natural resources (Pethybridge et al., 2020).

Like environmental management, ecological indicators have also been developed to represent the status of the whole ecosystem (Fulton et al., 2005; Shin and Shannon, 2010). Ecological indicators can synthesize information about the biotic and abiotic interactions revealing the status of ecosystem functioning, stability, development and stress (Niquil et al., 2012). Thus, the application of ecological indicators to diagnose ecosystems is beneficial not only for the scientific relevance but also for management purposes (Tam et al., 2017). One example is the evaluation of fishery management, which may benefit from the development of indicators. Several indicators stemming from multiple ecosystem models have been applied to evaluate fishing scenarios, as well as the impact of actual fishing pressure, on many marine ecosystems worldwide (Shannon et al., 2014; Coll et al., 2016; Britton et al., 2019). These studies show that the indicators are useful to support not only the ecosystem assessments but also interpretation of outputs generated by scenarios depicted in ecosystem models. In order to advance knowledge on ecosystem functioning, it is essential to understand the food web network and the organization of energy flows, since fishery induces changes in the structure of marine ecosystems (Pauly et al., 1998). Network-derived indices consider whole systems, being able to demonstrate how disturbances affect the structure, functioning and resilience of ecosystems (Fath et al., 2019; Safi et al., 2019). Thus, network-derived indicators, which have not been studied in this context yet, are promising candidates for determining GES (de la Vega et al., 2018). Moreover, these indicators may further clarify the differences between ecosystem models, by providing information on the architecture of the food web network and other assumptions that could affect the models outputs.

In this study, we used two ecosystem models to simulate fishing pressure for unraveling its impacts on the food web. We simulated gradients of three different fishing mortality scenarios using Atlantis and OSMOSE models applied to the Eastern English Channel ecosystem. A selection of outputs of these models were used as parameters for ecological network analysis (ENA; Ulanowicz, 2004). The ENA provides network-derived indicators based on qualitative and quantitative analysis of energy flows. We analyzed the performance of a set of these indicators across a range of fishing scenarios, to understand their response to fishing mortality and to evaluate their robustness to model structure and fishing strategies. This study is a first step to explore network indicators computed from weighted food webs of two ecosystem models calibrated for the same ecosystem.

2. Material and methods

2.1. Study site

The Eastern English Channel (EEC) is an important habitat for economically relevant species, which are exposed to intense harvest by fisheries (Marchal and Vermard, 2022). The EEC is characterized by shallow (50 m average depth) and well-mixed waters. These particular features enhance the use of benthic resources as energy provider for the whole food web, triggering benthic-pelagic coupling (Kopp et al., 2015; Giraldo et al., 2017; Cresson et al., 2020). The EEC ecosystem has been extensively studied, including through the use of different ecosystem modeling approaches, i.e. Ecopath with Ecosim (Metcalfe et al., 2015), Atlantis (Girardin et al., 2018), and OSMOSE (Travers-Trolet et al., 2019). The site represents an interesting case study, since several models based on different hypotheses are available and could be used in combination to capture the complexity of ecosystem functioning (Travers-Trolet et al., 2019). The Ecopath with Ecosim (EwE) model from the EEC was not included in this study because the parameters of the model are not available in the EcoBase database (<https://ecobase.ecopath.org>).

Moreover, the time series data used to calibrate the EwE model (1973–2006) was from a different period in comparison to Atlantis and OSMOSE and it relied mainly in information from surrounding ecosystem. Therefore, in this study, we focused on Atlantis and OSMOSE ecosystem models that were previously calibrated and validated (Girardin et al., 2018; Travers-Trolet et al., 2019). These models were used to compute network-derived indicators through the application of ecological network analysis (ENA).

2.2. Atlantis

Atlantis is a deterministic and spatially resolved model (Fulton et al., 2004, 2011; Audzijonyte et al., 2019) that relies on the physical and fishing modules that are coupled with ecological trophic interactions. The dynamics of the system, depicted on three-dimensional irregular polygons (i.e. representing depth in layers along the area covered), consider ecological processes (predation, natural mortality, reproduction, recruitment, growth), fishing activity (including information on fishing mortality, effort and types of fleets and métiers) and the hydrodynamics of the area (e.g., tides and inflow of organic matter originated from rivers or adjacent areas). The Atlantis EEC model was calibrated on the period 2002–2011 using data collected from scientific surveys sampling, commercial fishing and literature (Girardin et al., 2018; Bracis et al., 2020). The functional groups in Atlantis EEC comprise 21 vertebrates, 16 groups of invertebrates and 3 groups of detritus. All functional groups were maintained in the ENA food web structure (Appendix - Fig. A.1a), except for detritus, which was considered as one single compartment in ENA by gathering the different types of detritus. Due to the demanding scenarios simulations, Atlantis was simulated for 60 years and the outputs of the last 5 years were used to carry out ENA. Indicators generated for the last 5 years were averaged to smooth the interannual variability. To construct the ENA, we used abundance of vertebrates, structural nitrogen, reserve nitrogen, biomass of invertebrates in mg N, specific mortality (i.e. predation and natural mortality) and catch outputs from Atlantis (Table 1; Appendix - Fig. A.2).

2.3. OSMOSE

OSMOSE is a spatially explicit individual-based model. It represents fish individuals from egg to adult stages, grouped into schools and defined by their size, weight, age, taxonomy and spatial position on a 2D regular grid (Shin and Cury, 2004). The trophic interactions between the modelled species depends on the size-based opportunistic predation based on the size adequacy and spatial co-occurrence between a predator and its prey. The OSMOSE model constructed for EEC was calibrated for the period 2000 to 2009 (Travers-Trolet et al., 2019). This model considered 14 fish species representing higher trophic levels and 10 low trophic levels compartments composed mainly by invertebrates (Travers-Trolet et al., 2019; Appendix - Fig. A.1b). Lower trophic levels were not explicitly modelled and were only used as prey fields for higher trophic level compartments; thus, the primary producers and invertebrates compartments were not receiving any energy flow. Their biomass distribution was forced by the outputs from the biogeochemical model ECO-MARS3D applied to the EEC (Travers-Trolet et al., 2019; Le Goff et al., 2017). Following Travers-Trolet et al. (2019), the model ran for 120 years to ensure the stabilization of the populations. Due to model stochasticity, we ran 15 replicates for each simulation. The ENA indicators generated from the last 20 years were averaged to smooth the interannual variability. The OSMOSE outputs used to construct the ENA were predator pressure, mortality rate by predation, abundance and biomass (Table 1; Appendix - Fig. A.3).

2.4. Fishing mortality scenarios

Fishery for both Atlantis and OSMOSE EEC models is implemented as

Table 1

Setting up of the energy flows for Atlantis, OSMOSE and modified Atlantis models to fit ENA (more details of the workflow are available in the Figures A.2 and A.3).

	Atlantis	OSMOSE	modified Atlantis
Time series period of model calibration	2002–2011	2000–2009	2002–2011
Intercompartmental exchange flows (tons · km ⁻² · day ⁻¹)	<ol style="list-style-type: none"> 1) Specific mortality by predation output was applied to infer energy flows proportions of the intercompartmental exchanges. 2) Biomass of vertebrate groups was obtained from abundance, structural (e.g., bones) and reserve (e.g., gonad, fat, muscles) nitrogen outputs. 3) Weighted energy flows resulted from the product of the energy flows proportion and biomass of each group. 4) Natural mortality of each species was considered as flow to detritus, which was a product of the relative biomass lost by natural mortality and the total biomass of each group. 5) Age classes of vertebrate groups were considered for calculating natural and predation mortality. However, for ENA purposes, age classes were removed to restrict the number of compartments. 	<ol style="list-style-type: none"> 1) The equation of OSMOSE for quantifying mortality by predation (N_{pred}) was calculated using initial abundance (N_i) and mortality rate by predation (M_{pred}) per time (t) in days. $N_{pred} = N_i \times (1 - e^{-M_{pred}}) \div t$ 2) N_{pred} was converted to biomass (B_{pred}) using the ratio initial prey biomass (B_i) over initial prey abundance (N_i). B_{pred} was represented per km², thus the area considered corresponds to the total ICES area VIII (35000 km²). $B_{pred} = N_{pred} \times \left(\frac{B_i}{N_i}\right) \div Area$ 3) The proportion of energy flow from prey to predator was inferred based on the predator pressure output of the model. 4) Intercompartmental exchange as weighted flow was a result from the product of the biomass corresponding to total mortality by predation and the proportion of energy flowing from prey to predator. 	The same procedure as Atlantis from 1 to 5
Detritus import	Model considers the nitrogen discharge from the rivers to EEC, these inputs were considered imports of energy (tons km ⁻² day ⁻¹) from outside the system to the detritus compartment	No detritus import was considered	The same procedure as Atlantis
Imports and exports	Whenever the outflow of a compartment was higher than its inflow, the ecological interpretation is that there is an excess of mortality (i.e. predation, natural and fishing mortality) or migration, which causes reduction in biomass. To compensate it, migrations of fish species and the inflow of phytoplankton and zooplankton were considered artificial imports of energy flowing into the system. By the other hand, the surplus of the inflows could represent biomass increase or transport of energy out of the system. Thus, the excess of compartments that received more energy flows than provided was considered as artificial exports	The low trophic compartments in OSMOSE are considered as static, these compartments provide energy to other trophic levels but do not exchange within themselves and do not vary in biomass. Thus, the import flows from primary producers and invertebrates were based on the supply of the low trophic level compartments to high trophic level. The surplus of the compartments flows represented by respiration and mortality (i.e. predation, natural and fishing mortality) was represented as exports out of the system	Migrations of fish species were considered as artificial imports or exports of energy. Whenever the outflow of detritus, primary producers and invertebrates was higher than the inflow, the surplus was considered as artificial import. Instead, whenever the outflow of any compartment was higher than the inflow, the surplus represented by respiration and mortality (i.e. predation, natural and fishing mortality) was considered as artificial export
Balancing method (Allesina and Bondavalli, 2003)	If the system was not balanced, the method applied was the AVG2, since it does not produce high variation on the indices compared to the other methods (Allesina and Bondavalli, 2003)	Since we were dealing with a specific case of ENA, i.e. the inflow from low trophic level compartments is unlimited, we were more concerned about preserving the outflows balance. Thus, we used the input or donor method (Allesina and Bondavalli, 2003) to balance the systems, whenever necessary	Since the detritus, primary producers and invertebrates were considered as energy donors, like OSMOSE, the balancing method used was input or donor method

constant fishing mortality per species or functional groups (Bracis et al., 2020; Travers-Trolet et al., 2019). The fishing mortality scenarios were designed to test different fishing strategies. The fishing strategies were defined according to the group of exploited species (Shin et al., 2018; Fu et al., 2018, 2019). Thus, the first fishing strategy scenario targeted high trophic level species (HTL), i.e. top predator species with a trophic level higher than 4. Trophic level information used for this classification is from Fishbase (Froese and Pauly, 2021) and previous studies in the area (Kopp et al., 2015; Giraldo et al., 2017; Cresson et al., 2020). Fish groups included were Atlantic cod, sharks, whiting, large bottom fish in Atlantis, and lesser spotted dogfish, whiting and cod in OSMOSE. The second scenario considered a gradual change of low trophic level species (LTL) fishing mortality, i.e. plankton-feeding forage fish species. The group selected to represent LTL scenario was Clupeidae as target forage species for Atlantis, and sardine and herring in OSMOSE. The third scenario included all trophic levels (ALL). In this scenario, change in fishing mortality was applied to all species relevant for fishery. Moreover, in each scenario, a multiplier λ was applied to the F_{MSY} (the fishing mortality at Maximum Sustainable Yield) (Fu et al., 2018). For all targeted fish species (equation (1)), it generated a fishing mortality gradient, from no catches ($\lambda = 0$) to twice the F_{MSY} level ($\lambda = 2$) with 0.2 intervals. The F_{MSY} of each target species was computed for Atlantis

through the reconstruction of the curve yield per fishing mortality; and followed Travers-Trolet et al. (2020) procedure that estimated F_{MSY} of the target species in OSMOSE. The species that were not targeted in the scenarios were fished at their calibrated fishing mortality.

$$F_{target\ species} = \lambda \times F_{MSY\ target\ species} \quad (1)$$

2.5. Ecological network analysis (ENA)

There are two main sources of information necessary to carry out ENA: who interacts with whom and how much. This information enables the construction of weighted food webs snapshots (Ulanowicz, 2004). The ENA is a method that analyzes energy flow of the interactions that consider living and non-living groups to provide a holistic overview on the structure and functioning of the ecosystem. The ENA provides metrics (e.g., information theory indices; Ulanowicz, 2001) that can be used as indicators of ecosystem status (Fath et al., 2019). The compartments of each food web were inherited from ecosystem models, and correspond to different levels of aggregation. The compartments' flows of energy are represented by imports, intercompartmental exchange, exports and respiration (or energy loss). All these flows were determined based on the outputs of the Atlantis and OSMOSE models (Table 1). As respiration is not provided by the models, respiration and exports were

considered as a single outflow (Fath et al., 2007). Moreover, the energy flows mobilized by fisheries were not allocated to specific compartments; instead, these flows were incorporated indistinctly to the exports. Once the compartments and weighted flows were set, we applied ENA to the networks using the package enaR (Borrett and Lau, 2014; <https://github.com/SEELab/enaR>) in R environment (R Core Team, 2021) to analyze the models' outputs and compute the network-derived indicators.

In order to carry out ENA on fully comparable networks, an additional Atlantis network was analyzed (referred to "modified Atlantis" hereafter). The food web structure output of Atlantis was aggregated to mimic the structure of OSMOSE in order to compare similar ecosystem components. The energy exchange of the detritus, primary producers and invertebrates corresponds to large amounts of all the energy flowing in the food web especially in EEC that enables benthic-pelagic coupling. Atlantis depicts such trophic interactions in depth, which may buffer the effects of increasing fishing mortality on the indicators. In OSMOSE, primary producers and invertebrates are considered as energy donors, i.e. these compartments are boxes and the exchange of energy between these compartments are not considered. Therefore, detritus, primary producers and invertebrates (except for cephalopods) compartments of Atlantis were maintained and considered as energy donors only in the modified Atlantis.

2.6. Ecological network indicators

The selection of indicators was based on previous literature. It justified a set of ENA indices compilation both suitable to inform policy makers and relevant to stakeholders (see de la Vega et al., 2018; Fath et al., 2019; Safi et al., 2019; Lewis et al., 2021), and also constrained by the characteristics of our models. In this study, we focused on indicators derived from network metrics and information theory given their ability to capture the architecture energy flows (quantitatively and qualitatively), and to measure the efficiency of the network and the resilience of the food webs. Indicators related to cycling (e.g., Finn cycling index) and Lindeman Spine, i.e. chain-like flows, (e.g., omnivory index, detritivory: herbivory ratios) were excluded from this study. They would not be realistic in OSMOSE because the model does not include non-living compartments and displays a large number of cycles, due to the opportunistic predation. Thus, the selected ENA indicators for this study were total system throughput (TST_p), average mutual information (AMI), flow diversity (H), overhead (OH), ratio between ascendancy and development capacity (or relative ascendancy; A/DC), ratio between redundancy and development capacity (or relative redundancy; R/DC), average path length (APL) and connectance (C) (Table 2).

2.7. Data analysis

The first step to evaluate differences between the indicators' behavior according to the ecosystem model and scenarios was to scale the data. The range of the indicators' values for each model differed, thus we normalized the data using z-score (Equation (2)) to better understand whether they would follow similar patterns along the fishing mortality gradient. The calculation considers the observed value, the mean μ and the standard deviation σ of the indicator for each scenario.

$$Z = \frac{x - \mu}{\sigma} \tag{2}$$

The second step was to analyze the trends and directions of the indicators along the fishing gradient. For this purpose, generalized additive models (GAM) were fitted to the variables to explore the indicators responses following Equation (3), where em refers to the ecosystem model and λ to the fishing mortality multiplier. The functions s₁ and s₂ refer to the smooth terms of the model (we implemented the thin plate regression spline).

Table 2

Information about the indicators selected stem from Finn (1976); Rutledge et al. (1976); Hirata and Ulanowicz (1984); Ulanowicz (2001, 2004); Martinez (1991); Scotti et al. (2009) and the equations were extracted from the enaR package (Borrett and Lau, 2014). Note that T_{ij} is the energy flow from compartment i to compartment j; T_i is the energy flow from compartment i to all other compartments connected to it; T_j is the energy flow from all compartments connected to j into compartment j; n is the number of compartments and n + 2 refers to the whole matrix of interactions (i.e. intercompartmental exchange, imports and exports); k is a scalar constant; z is the energy import from outside the network to the compartments. Note that TST_{flow} is the sum of the flows entering (or leaving) each compartment..TST_{flow} = ∑_{i=0}ⁿ⁺² ∑_{j=0}ⁿ⁺² T_i

Indicators	Equation	Definition and relevance
Total System Throughput (TST _p)	$TST_p = \sum_{i=0}^{n+2} \sum_{j=0}^{n+2} T_{ij}$	Total amount of energy flowing through a system. Inform how the size and activity of the ecosystem behave to fishing pressure
Average mutual information (AMI)	$AMI = k \sum_{i=0}^{n+2} \sum_{j=0}^{n+2} \left(\frac{T_{ij}}{TST_p} \right) \cdot \log_2 \left(\frac{T_{ij} \cdot TST_p}{T_i \cdot T_j} \right)$	Configuration of the energy flows through the system. Demonstrate changes in the complexity of the network, (i.e. in the efficiency of the system to transport energy)
Flow diversity (H)	$H = - \sum_{i=0}^{n+2} \sum_{j=0}^{n+2} \frac{T_{ij}}{TST_p} \cdot \log_2 \left(\frac{T_{ij}}{TST_p} \right)$	The number and diversity of flows embedded in the TST _p . Indicate if the flows are more evenly distributed in quantity of energy and quantity of interactions
Overhead (OH)	$OH = \sum_{i=0}^{n+2} \sum_{j=0}^{n+2} T_{ij} \cdot \log_2 \left(\frac{T_{ij}^2}{T_i T_j} \right)$	The amount of non-organized energy flows occurring in the system. Indicate changes in amount of parallel flows in the food web under fishing pressure
Development capacity (DC)	$DC = TST_p \cdot H$	Upper limit of development of an ecosystem, which derives from flows diversity (H) and ecosystem activity (TST _p). This indicator is described because it is used in the following two indicators to normalize scores of flow organization and redundancy
Relative ascendancy (A/DC)	$\frac{A}{DC} = TST_p AMI \div DC$	Proportion of organized complexity within a system. Higher values indicate lower degrees of freedom in energy circulation, assuming that organization is related to a lower amount of parallel

(continued on next page)

Table 2 (continued)

Indicators	Equation	Definition and relevance
Relative redundancy (R/DC)	$R/DC = \frac{OH_i}{DC}$	flows, making the system more efficient (but also more rigid) to transport energy. Redundancy is represented by relative internal overhead (OH _i), i.e. parallel flows. The proportion of redundant flows within a system. Express the resilience of the system, since the parallel flows increase the chances of a system to recover from and withstand disturbance.
Average path length (APL)	$APL = \frac{TST_{flow}}{\sum_{i=1}^n z}$	Average number of steps that the input of one unit of energy will circulate before leaving the system. Related to the ability of the system to use and exchange energy among compartments.
Connectance (C)	$C = \frac{n \text{ of links}}{n \text{ of compartments}^2}$	Density of possible links occurring in a network. Indicate if the disturbances would result in lower connectivity between the groups.

$$Indicator = \beta_0 + s_1(\lambda) + s_2(\lambda) \bullet em + \varepsilon, \quad \varepsilon \sim N(0, \sigma^2) \quad (3)$$

The analysis was carried out in R environment (version 4.0.5; R Core Team, 2021) using the R package “mgcv” (version 1.8–34; Wood, 2017).

3. Results and discussion

The network-derived indicators revealed the complexity of the trophic interactions depicted in each modeling approach, and demonstrated that each fishing strategy from each model may produce particular responses to the structure of the simulated food web. Nevertheless, the network indicators computed from the simulations of OSMOSE and Atlantis shed light on how energy flow of food webs is distributed along fishing mortality gradients.

3.1. Comparison between the models

The network indicators are known to be specific to ecosystems and architecture of the food web. Thus, beside the responses to the fishing pressure, it was expected that the indicators would depend to some extent on ecosystem models, due to the main assumptions of each model, which could affect the structure of the food web and the distribution of the energy flows. There are three main considerations about the complexity of the food webs construction to compare the indicators computed from the models outputs.

First, the trophic interactions depicted in each model are different. Atlantis implements a whole ecosystem approach, i.e. it considers the trophic interactions of the whole food web. The bottom compartments of the food web (detritus, primary producers and invertebrates) are exchanging energy between themselves and with high trophic levels

compartments like fish, mammals and birds (Girardin et al., 2018). Instead, OSMOSE focuses on the trophic interactions of a selected group of fish. The primary producers and invertebrates are represented as forcing compartments that provide energy for the high trophic level species without interaction between themselves. Total system throughput (TSTp) demonstrates that the quantity of energy flowing within the depicted system was higher for Atlantis than OSMOSE (Fig. 1). This result is attributed to the energy circulating in, out and within the low trophic compartments (i.e. invertebrates, phytoplankton and detritus) in Atlantis. The energy flowing into the low trophic compartments accounts for 83.86 % of the total amount of energy flow of the whole system simulated in Atlantis model. The TSTp revealed that the primary producers, invertebrates and non-living compartments may mobilize a considerable amount of energy, which was expected since strong benthic-pelagic coupling has been detected in numerous empirical and modeling studies in the EEC (Kopp et al., 2015; Giraldo et al., 2017; Cresson et al., 2020; Bracis et al., 2020). Moreover, benthic invertebrates and their dependence on the detritus play an important role on providing energy to the EEC food web (Giraldo et al., 2017). This process is captured by Atlantis (Girardin et al., 2018; Bracis et al., 2020) and not by OSMOSE. The removal of trophic interactions of the invertebrates, primary producers and detritus from Atlantis outputs resulted in TSTp values (Fig. 1) comparable to OSMOSE ones.

Second, the presence and absence of a detritus compartment may reflect on the indicators. Detritus (i.e. non-living compartments) is connected to a large number of compartments and exchanges great amounts of energy in the food web, thus it is an important hub for energy recycling. Although Atlantis includes three functional groups for detritus, the detritus was condensed in one non-living compartment for ENA purposes. As there is no detritus compartment represented in OSMOSE, the ENA was carried out using OSMOSE outputs without a non-living compartment. Network indicators are sensitive to the aggregation of non-living groups of the food web (Allesina et al., 2005). The indicator relative ascendancy (A/DC) is known to decrease with the aggregation of detritus groups (Allesina et al., 2005). Although, in this study we dealt with presence and absence of detritus, we observed that the absolute value of A/DC of OSMOSE was lower than both versions of the networks derived from Atlantis (in the Atlantis modified, A/DC is slightly lower than Atlantis) (Fig. 1).

The third consideration is that the aggregation and exclusion of compartments from the food web influence network indicators (Abarca-Arenas and Ulanowicz, 2002; Johnson et al., 2009). The food web compartments and structures of Atlantis and OSMOSE calibrated for the EEC are different. The network constructed with Atlantis outputs has 38 compartments that include not only fish, but also marine mammals, birds, invertebrates, primary producers and detritus. Instead, the OSMOSE-based network displays lower resolution containing 24 compartments. OSMOSE focuses mostly on higher trophic level species (fish groups) that occur in the EEC ecosystem (Travers-Trolet et al., 2020). The increase of compartments may result in increase of A/DC and decrease of R/DC (Johnson et al., 2009), as observed in our results (Fig. 1). Thus, the higher value of A/DC in Atlantis may also be an effect of the number of compartments, beside the presence of detritus as mentioned above. The number of compartments also affect the level of organization of the system, which may have been captured by the indicators of energy flows diversity (H), average mutual information (AMI) and overhead (OH). These indicators reveal the complexity of the interactions of the network by indicating how orderly and coherently the energy flows connections are, AMI denotes organization of the flows (i.e. specialized flows) of a system while H represents the evenness of the flows distribution and OH the amount of unorganized flows from the system's capacity (Ulanowicz, 2004). In OSMOSE, H and AMI are higher compared to the outputs of Atlantis, conversely OH is lower for OSMOSE in comparison to Atlantis (Fig. 1). Moreover, these indicators computed from the modified Atlantis tend show values closer to OSMOSE (Fig. 1), which suggests that the organization of the flows from Atlantis was also

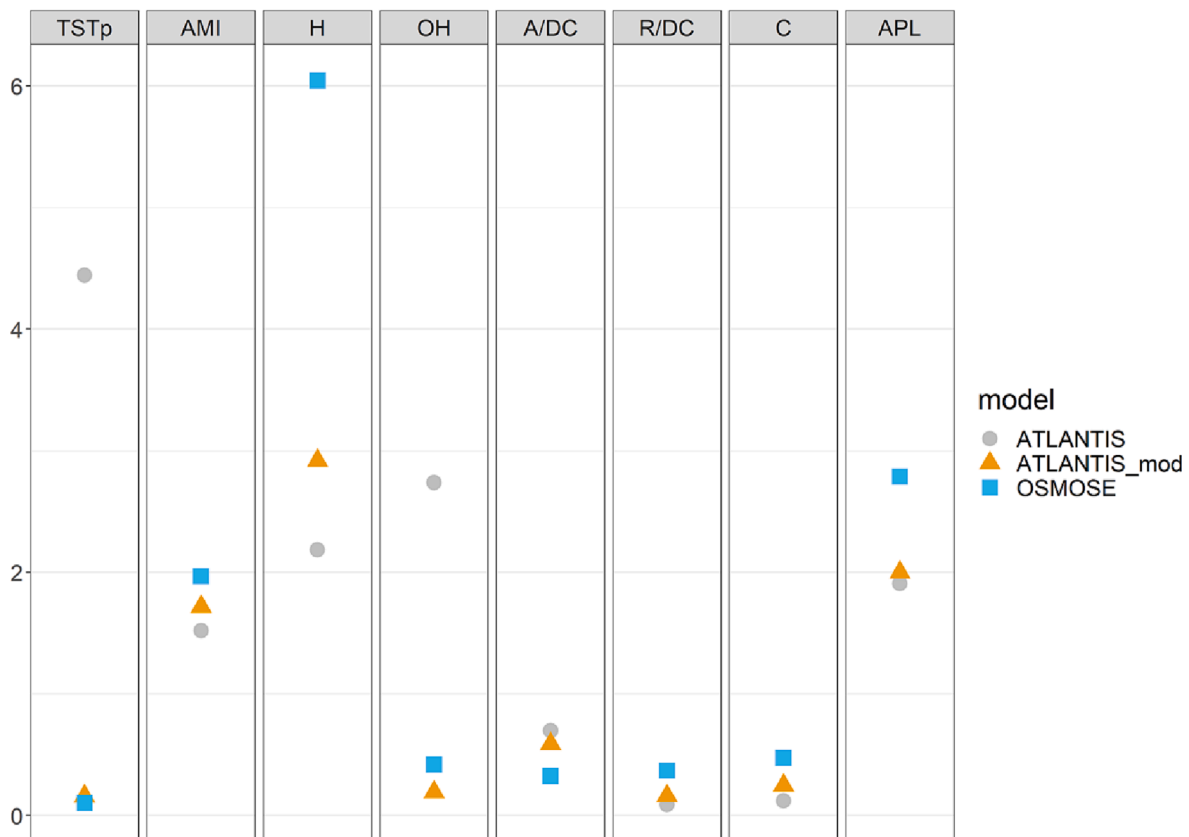


Fig. 1. Network indicators derived from the ENA computed from the outputs of the ecosystem models. The columns represent the absolute values of the indicators: total system throughput (TSTp) in $\text{ton} \cdot \text{km}^{-2} \cdot \text{day}^{-1}$, average mutual information (AMI), flow diversity (H), overhead (OH) in $\text{ton} \cdot \text{km}^{-2} \cdot \text{day}^{-1}$, relative ascendency (A/DC), relative redundancy (R/DC), average path length (APL) and connectance (C). The indicators of Atlantis were computed with the original trophic interactions (grey circles). In addition, the energy flows of Atlantis were modified, i.e. primary producers and invertebrates compartments were considered as energy donors for higher trophic level compartments (yellow triangles). The OSMOSE indicators were computed after the original trophic interactions of the model outputs (blue squares). (For interpretation of the references to color in this figure legend, the reader is referred to the web version of this article.)

strongly related to the trophic interactions controlled by the detritus, primary producers and invertebrates. In this context, we should interpret these results as indicators of complexity of the food web interactions of the models. In OSMOSE, the flows are running through fewer pathways and the amount of parallel flows is higher in comparison to Atlantis as indicated by AMI and OH (Fig. 1), this pattern may be explained by the number of compartments of the models (Johnson et al. 2009). However, the diversity of the flows (H) remains higher in OSMOSE rather than Atlantis. These results demonstrate the differences in the energy flow structure and magnitude between the two models. The energy flow is also a product of the assumptions of the models for predation. Feeding preference of Atlantis is pre-defined whereas it emerges from the opportunistic predation in OSMOSE. Even though Atlantis considers mouth-gape limitations for predation, it also relies on a prey availability matrix, which makes the feeding less flexible than OSMOSE. The opportunistic feeding behavior simulated in OSMOSE is based on body size, thus it generates more cycles, increasing the connectivity between predators and preys (Smith et al., 2015). Such characteristics drove the higher values of the average path length (APL) in OSMOSE food web compared to Atlantis (Fig. 1). In addition, Johnson et al. (2009) found that less compartments increases APL and connectance (C). The indicator C corresponds to the ratio of connections density and number of groups. Thus, beside the amount of connections generated by the energy recycling, the quantity of groups present in the models explains the higher C values in OSMOSE in comparison to Atlantis (Fig. 1). Although the indicators seem contradictory, they reveal that the feeding feature of OSMOSE generates several interactions; however the amount of energy flowing through the main paths is

preserved.

3.2. Comparison between fishing mortality scenarios

3.2.1. Size and activity of the system

The energy flow mobilized by fish groups resulted in lower activity of the ecosystem under the fishing mortality gradient. The TSTp indicator (i.e. size of the ecosystem and amount of energy flowing in the system) computed from OSMOSE responded to ALL, HTL and LTL scenarios showing a decrease on the energy flow in relation to the fishing mortality gradient. While TSTp exhibited very little variation when calculated from Atlantis (Fig. 2; Table 3), there were similarities in the directions of the trends in the modified Atlantis in comparison to OSMOSE (Fig. 2; Table A1). This result demonstrates that the interactions of the invertebrates, primary producers and detritus compartments depicted in Atlantis buffered the response of the indicator, as discussed previously. The decrease of energy flowing in the system was expected with the removal of fish biomass and was detected before (Mukherjee et al., 2015).

3.2.2. Organization of the energy flows of the system

The efficiency of the network to transport energy increased and the diversity of flows decreased along fishing mortality gradient. The increasing intensity of fishing mortality on low trophic level fish groups led to an increase of AMI in scenario LTL (Fig. 2, Table 3). This indicates that the removal of forage fish groups constrained the energy flows to fewer paths in the network (Scotti et al. 2009). The responses of the AMI to fishing mortality were stronger for the outputs from OSMOSE than

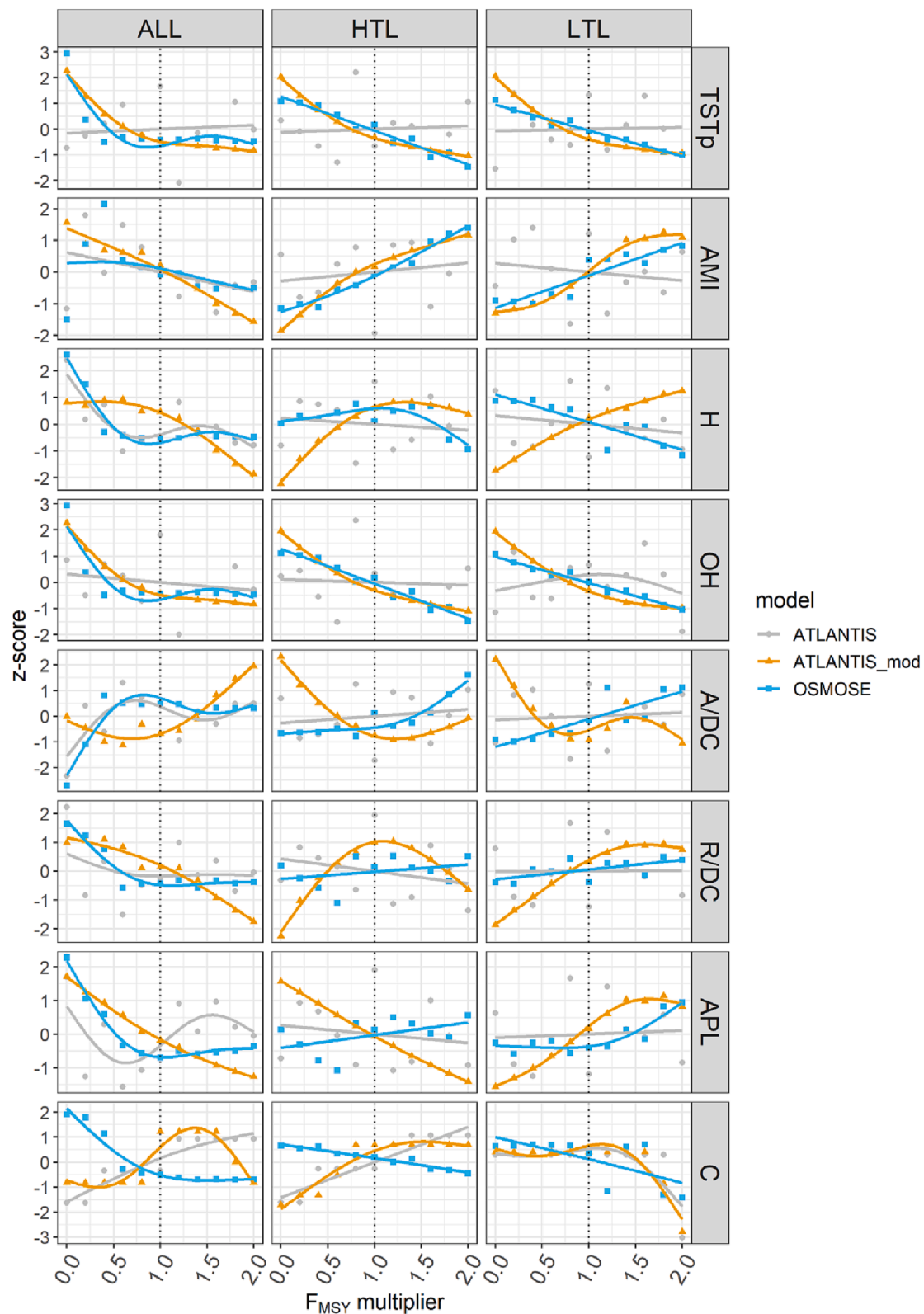


Fig. 2. GAM fitted to a gradient of fishing pressure (F_{MSY} multiplier; i.e. λ). Each column represents a fishing scenario. The fishing scenario (ALL) simulates the fishing mortality gradient over all exploited species, while the other two scenarios considers only high trophic level species (HTL) and low trophic level species (LTL). The rows represent the network-derived indicators normalized using z-score: total system throughput (TSTp), average mutual information (AMI), flow diversity (H), overhead (OH), relative ascendancy (A/DC), relative redundancy (R/DC), average path length (APL) and connectance (C). Grey circle and yellow triangle correspond respectively to the indicators computed from the original and modified versions of Atlantis food webs and the blue square corresponds to OSMOSE. (For interpretation of the references to color in this figure legend, the reader is referred to the web version of this article.)

Table 3

Summary statistics of the GAM fitted to the indicators computed from the outputs of Atlantis, modified Atlantis and OSMOSE after the simulation of fishing scenarios represented in the columns. Effective degrees of freedom (edf), reference degrees of freedom (Ref.df), F-value (F), significance of the smooth terms (p-value), adjusted R-squared (R-sq.(adj)), explained deviance (Dev. explained). The fishing scenario (ALL) simulates the fishing mortality gradient over all exploited species, while the other two scenarios considers only high trophic level species (HTL) and low trophic level species (LTL). The indicators represented are total system throughput (TSTp), average mutual information (AMI), flow diversity (H), overhead (OH), relative ascendency (A/DC), relative redundancy (R/DC), average path length (APL) and connectance (C).

TSTp	scenario ALL				scenario HTL				scenario LTL			
	edf	Ref.df	F	p-value	edf	Ref.df	F	p-value	edf	Ref.df	F	p-value
s(λ)	1.00	1.00	0.22	0.64	1.00	1.00	7.58	0.01*	1.00	1.00	61.45	<0.01*
s(λ):ATLANTIS	6.11E-06	1.22E-05	0.11	1.00	7.69	8.57	4.93	<0.01*	8.32	8.87	16.61	<0.01*
s(λ):ATLANTIS_mod	1.87	2.34	5.38	<0.01*	1.13	1.66	1.90	0.21	2.72	3.39	5.72	<0.01*
s(λ):OSMOSE	2.87	3.57	3.84	0.02*	1.00	1.00	0.16	0.69	1.79E-05	3.57E-05	8.00E-03	1.00
R-sq.(adj)	0.48				0.82				0.91			
Dev. explained	60.60 %				89.30 %				94.70 %			
AMI												
	edf	Ref.df	F	p-value	edf	Ref.df	F	p-value	edf	Ref.df	F	p-value
s(λ)	1.00	1.00	4.25	0.05	1.00	1.00	0.94	0.34	1.00	1.00	11.89	<0.01*
s(λ):ATLANTIS	2.85	3.75	3.69	0.03*	5.10E-05	1.02E-04	2.00E-03	1.00	1.65	2.05	4.93	0.01*
s(λ):ATLANTIS_mod	1.00	1.00	8.68	<0.01*	1.00	1.00	7.92	<0.01*	1.00	1.00	1.08	0.31
s(λ):OSMOSE	4.90	5.99	4.47	<0.01*	1.00	1.00	6.68	0.01*	1.13E-05	2.25E-05	0.03	1.00
R-sq.(adj)	0.71				0.57				0.51			
Dev. explained	81.40 %				63.50 %				59.60 %			
H												
	edf	Ref.df	F	p-value	edf	Ref.df	F	p-value	edf	Ref.df	F	p-value
s(λ)	1.00	1.00	8.34	<0.01*	2.05	2.42	3.21	0.04*	1.00	1.00	1.12	0.30
s(λ):ATLANTIS	3.51	4.53	6.40	<0.01*	1.00	1.00	4.10	0.05	4.31E-06	8.62E-06	0.11	1.00
s(λ):ATLANTIS_mod	2.47	3.08	4.11	0.02*	0.60	0.97	3.00E-03	0.95	1.00	1.00	17.58	<0.01*
s(λ):OSMOSE	3.88	4.79	8.42	<0.01*	1.00	1.00	4.57	0.04*	1.00	1.00	2.68	0.11
R-sq.(adj)	0.86				0.39				0.50			
Dev. explained	91.40 %				51.70 %				57.40 %			
OH												
	edf	Ref.df	F	p-value	edf	Ref.df	F	p-value	edf	Ref.df	F	p-value
s(λ)	2.00	2.38	8.07	<0.01*	1.00	1.00	95.64	<0.01*	1.00	1.00	475.00	<0.01*
s(λ):ATLANTIS	1.00	1.00	4.84	0.03*	8.41	8.91	15.38	<0.01*	8.88	9.00	145.86	<0.01*
s(λ):ATLANTIS_mod	2.92E-04	5.43E-04	1.50E-02	1.00	2.35	2.93	2.61	0.09	3.87	4.78	28.91	<0.01*
s(λ):OSMOSE	2.29	2.85	1.31	0.38	1.89E-05	3.77E-05	6.00E-03	1.00	4.81E-06	9.63E-06	0.07	1.00
R-sq.(adj)	0.48				0.91				0.99			
Dev. explained	60.10 %				94.70 %				99.40 %			
A/DC												
	edf	Ref.df	F	p-value	edf	Ref.df	F	p-value	edf	Ref.df	F	p-value
s(λ)	1.00	1.00	6.60	<0.01*	1.96	2.33	5.31	0.01*	1.00	1.00	0.18	0.67
s(λ):ATLANTIS	3.10	4.06	4.92	<0.01*	1.00	1.00	2.26	0.15	1.72E-05	3.44E-05	0.10	1.00
s(λ):ATLANTIS_mod	2.74	3.41	5.25	<0.01*	2.03	2.53	9.80	<0.01*	2.82	3.51	3.37	0.02*
s(λ):OSMOSE	3.83	4.74	6.12	<0.01*	2.28E-05	4.24E-05	0.03	1.00	1.00	1.00	3.76	0.06
R-sq.(adj)	0.75				0.47				0.39			
Dev. explained	85.10 %				58.90 %				52.20 %			
R/DC												
	edf	Ref.df	F	p-value	edf	Ref.df	F	p-value	edf	Ref.df	F	p-value
s(λ)	1.00	1.00	2.22	0.15	1.00	1.00	0.42	0.52	1.60	1.93	5.76	0.01*
s(λ):ATLANTIS	4.55	5.58	4.20	<0.01*	1.00	1.00	0.87	0.36	1.00	1.00	6.11	0.02*
s(λ):ATLANTIS_mod	1.46	1.78	0.40	0.70	1.72	2.38	6.21	<0.01*	0.29	0.51	0.01	0.96
s(λ):OSMOSE	1.51	2.12	4.11	0.03*	1.00	1.00	0.21	0.65	1.00	1.00	3.57	0.07
R-sq.(adj)	0.73				0.34				0.38			
Dev. explained	82.00 %				48.20 %				49.20 %			
APL												
	edf	Ref.df	F	p-value	edf	Ref.df	F	p-value	edf	Ref.df	F	p-value
s(λ)	1.57	1.88	5.74	0.01*	1.00	1.00	0.69	0.41	1.00	1.00	0.06	0.81
s(λ):ATLANTIS	4.12	5.23	5.18	<0.01*	1.23E-05	2.46E-05	0.00	1.00	0.58	0.95	0.26	0.62

(continued on next page)

Table 3 (continued)

TSTp	scenario ALL				scenario HTL				scenario LTL			
	edf	Ref.df	F	p-value	edf	Ref.df	F	p-value	edf	Ref.df	F	p-value
s(λ):ATLANTIS_mod	1.00	1.00	4.43	0.04*	1.00	1.00	7.81	<0.01*	1.00	1.00	5.65	0.02*
s(λ):OSMOSE	2.80	3.49	4.70	<0.01*	1.00	1.00	2.06	0.16	1.35	1.61	1.25	0.41
R-sq.(adj)	0.81				0.39				0.41			
Dev. explained	87.90 %				48.10 %				51.90 %			

C	scenario ALL				scenario HTL				scenario LTL			
	edf	Ref.df	F	p-value	edf	Ref.df	F	p-value	edf	Ref.df	F	p-value
s(λ)	1.00	1.00	7.78	0.01*	1.00	1.00	134.40	<0.01*	2.77	2.95	11.02	<0.01*
s(λ):ATLANTIS	1.07	1.58	0.90	0.34	8.27	8.86	105.80	<0.01*	1.81E-05	3.48E-05	0.09	1.00
s(λ):ATLANTIS_mod	4.93	6.02	10.07	<0.01*	7.36	8.36	116.30	<0.01*	1.00	1.00	0.26	0.62
s(λ):OSMOSE	3.06	3.80	13.04	<0.01*	0.00	0.00	0.00	1.00	1.51	1.86	0.28	0.70
R-sq.(adj)	0.89				0.99				0.60			
Dev. explained	92.80 %				99.40 %				69.00 %			

Atlantis, representing the replacement of the interrupted flows by energy flows in the low trophic level compartments. Thus, AMI computed from OSMOSE became more comparable with modified Atlantis. Flow diversity (H) declined in both models under scenario ALL (Fig. 2), although there were differences between the shapes of the trends (Table 3). The relative ascendancy (A/DC) increased for both models in scenario ALL. The trend of A/DC differs between the models since it increases sharply up to 0.6 time F_{MSY} , and beyond this fishing mortality the trend of the indicator remained relatively high and stable in OSMOSE and Atlantis, while in modified Atlantis the trend sharply increases after F_{MSY} multiplier ≥ 1 (Fig. 2). The response curves of the indicators H and A/DC were not linear, according to the edf values (Table 3); however, they overlap respectively the directions of the trends along fishing mortality gradient in both models (Fig. 2). Although the relative redundancy (R/DC) displayed a decrease along the fishing mortality gradient in both models (Fig. 2), the trend was not significant in scenario ALL (Table 3). In HTL scenario, the outputs of both models yielded significant response of H and A/DC, and negligible response of R/DC in (Table 3). In the LTL scenario, these indicators did not present a clear or significant response, except for R/DC (Fig. 2, Table 3). The indicator OH computed from Atlantis did not respond strongly to the fishing mortality gradient, however it became comparable to OSMOSE once the bottom trophic levels were simplified in modified Atlantis (Fig. 2). The OH indicator decreased whenever the food web was exposed to the fishing mortality scenarios (Fig. 2, Table 3). The simplification of the network was confirmed by OH throughout the fishing scenarios, it indicated that the energy flowing in parallel pathways decreased along the gradient.

The structure of the energy flows was sensitive to the fishing mortality. Average path length (APL) responded to scenario ALL of fishing mortality (Table 3). The trend for the outputs of OSMOSE showed a sharp decline up to 0.8 time F_{MSY} while Atlantis displayed a mild increase (Fig. 2). Although the shape of the APL trend from modified Atlantis differs from OSMOSE (edf, Table 3), the declining trend of the indicator in relation to fishing mortality gradient is confirmed (Fig. 2). The indicator did not respond significantly to scenarios HTL and LTL except for modified Atlantis (Table 3). The connectance (C) responded significantly to all the fishing scenarios (Table 3). Interestingly, the indicator C displayed diverging trends for the outputs of OSMOSE and Atlantis in scenario ALL and HTL (Fig. 2). The Atlantis-derived indicator showed an increasing trend while it decreased for OSMOSE outputs. This response might also be explained by the different assumptions of OSMOSE and Atlantis models. The stochasticity of OSMOSE recruitment increases the probability of some fish groups extinction in response to the increasing fishing mortality in the simulations (Figure A.4). The removal of compartments by extinction decreases the connectivity of food webs (Saint-Béat et al., 2015), as observed in OSMOSE for all

scenarios. By the other hand, Atlantis relies on stock-recruitment relationships that lowered the probability of functional groups extinction, which explains the differences with OSMOSE in ALL and HTL scenarios. Regardless, the scenario LTL imposed a decreasing trend on C derived from both models meaning that the removal of the forage fish groups jeopardize the connections of the food web (Fig. 2). The combination of the APL and C shows that the removal of fish species led to loss of links that composed the trophic interactions in OSMOSE. The scenario ALL shortened the number of paths of the energy circulation while in HTL and LTL the energy was circulating more within the food web before leaving the system. This means that the even though the scenarios HTL and LTL decreased the connectivity of the trophic network, the energy that entered the system increased the number of steps before leaving. Instead, in scenario ALL, both energy pathways and food web connectivity decreased. Thus, the removal of all target fish species is more detrimental to the system.

The indicators revealed the simplification of the energy flows architecture due to fishing from the ecosystem that transitioned from a web-like to a chain-like structure. This change was not only qualitative (i.e. rupture of interactions) but also quantitative (i.e. decrease of interactions strength evenness). The amount of energy circulating in the system decreased and there was qualitative and quantitative simplification of the trophic interactions as fishing pressure increased (Fig. 2). Both models highlighted the fact the structure and the functioning of EEC ecosystem are sensitive to the level of fishing pressure. This result is in line with previous studies on the impact of fish removals on energy fluxes in the food web (Vasas et al., 2007; Funes et al., 2022).

3.2.3. Ecological perspective of the scenarios response

Different fishing strategies have already been demonstrated to modulate ecological indicators (Halouani et al., 2019; Fu et al., 2020). Besides the sensitivity to the food web structure provided by the models, the response of network indicators is also attributed to the variable levels of the fishing mortality scenarios. The deviance explained by the GAMs fitted for the indicators as a response to the gradient (Table 3) tended to be higher for most indicators computed from the scenario ALL in comparison to scenarios HTL and LTL with few exceptions (i.e. TSTp and OH). This result corroborates the findings for other ecological indicators previously studied that responded more clearly after they were computed from the simulation of similar ALL scenario (Fu et al., 2020). This scenario caused the simplification of the food web interactions as indicated by TSTp, OH and A/DC. This outcome was expected since overfishing on different trophic levels has already impaired the resilience of the ecosystem in other regions (Froese et al., 2022). In OSMOSE, cod and whiting groups collapsed in the scenario ALL (Figure A.4). Previous empirical results explained the abundance of whiting in the English Channel by the ability of this species to exploit energy flowing

from both benthic and pelagic pathways (Cresson et al., 2020; Timmerman et al., 2020). Therefore, the indicators seem to capture the effects of the extinction of cod and whiting (that occurred before the F attained the F_{MSY} ; Figure A.4) on energy flow through the steep decline of the TSTp and OH trends (Fig. 2). Apex predators are responsible for maintaining the biodiversity in ecosystems (Sergio et al., 2006). Thus, it was expected that the fishing pressure on top predators in scenario HTL would have strong impacts on network indicators because top-down control is a relevant mechanism to sustain the balance of food webs (Borer et al., 2006). Our results indicated that there was a decline of the amount of energy flow (TSTp) and a simplification of the network structure (decrease of OH) in the ecosystem under the HTL scenario. Nevertheless, the indicators sensitivity was slightly lower for HTL in comparison to the LTL scenario ones (R-sq adj.; Table 3). The impacts on the trophic interactions caused by the exploitation of forage species might intensify other trophic pathways as shown by APL (Fig. 2), since predators may have to find other sources of food. Moreover, the removal of LTL groups may have functional implications, for instance the benthic contribution to the food web that was enhanced in both models (Figure A.5). Indeed, forage species play a pivotal role in mediating energy circulation in food webs and represent a bottleneck to make energy flow of the planktonic food chain available to high trophic level groups (Piatt et al., 2020). Therefore, the whole-ecosystem effects of energy flows disruption caused by the decline on forage species could be stronger than the one triggered by the removal of apex predators.

3.3. A summary of the indicators

Each fishing scenario may cause different ecological impacts on the ecosystem; however, some network indicators were sensitive to the changes in the whole system for all the scenarios. The indicator OH was coherent between models and scenarios, although its responses to HTL and LTL scenarios were milder for Atlantis. One further indicator that showed strong responses in all three fishing scenarios was found in the modified Atlantis model: TSTp (Table A1). The indicators in HTL and LTL presented more linear responses than in scenario ALL. The indicators of scenario ALL were not linear and reached a plateau denoting that they might have attained a saturation point for the ecosystem response to fishing mortality. Nevertheless, the direction of the trends increased or decreased in the same way as in HTL and LTL. In general, TSTp and OH decreased when the ecosystem was exposed to stress due to fishing mortality (Table 4).

3.4. Caveats

Ecological interactions are also driven by environmental variability. Many of observed ecological communities are characterized by a strong seasonal variability due to biotic and abiotic fluctuations. There are few empirical studies on the seasonal variation of trophic functioning in the Eastern English Channel that could be included as parameters in the models. The available results show that species trophic plasticity may buffer temporal variability effects (Timmerman et al. 2021). However, the configuration of the community composition (i.e. species turnover) that oscillates due to migration patterns modifies the configuration of species interactions (Thompson et al. 2012). Therefore, seasons may affect the structure of the food webs influencing its complexity by modifying the energy flows between the different components of the ecosystem (Saavedra et al. 2016). Our study did not explore seasonality patterns, since our objective was to compare the fishing scenarios. Nevertheless, it would be interesting that in the future some effort is made to compare seasonal fishing impacts on the food webs.

Despite the benefits of using network indicators, one should bear in mind that their responses may be specific to model and region. It is crucial to have tests showing how the indicators behave under different levels of stress or throughout space and time (Fath et al., 2019), to identify the patterns that determine deviation from a healthy ecosystem.

Table 4

Summary of the responses of each indicator to the models, fishing strategy and direction of the response once the food web was exposed to increased fishing pressure. Red arrows mean that the indicator decreased in all scenarios and models, while the grey ones indicate that the direction was not coherent among all models and/or scenarios. The network-indicators represented are total system throughput (TSTp), average mutual information (AMI), flow diversity (H), overhead (OH), relative ascendency (A/DC), relative redundancy (R/DC), average path length (APL) and connectance (C).

Indicator	Model	Fishing strategy	Indicator trend in response to fishing pressure
TSTp	In Atlantis the indicator was buffered by the activity of low trophic level compartments. Once the interactions between low trophic compartments were removed (modified Atlantis), the indicator responded similarly	The direction of the response was coherent between the scenarios, unlike the shape of the curves	↓
AMI	The indicator was coherent when comparing OSMOSE with modified Atlantis	The fishing strategy generated different response directions for the scenarios. Scenario ALL led to a decrease while scenarios HTL and LTL increased AMI	↓
H	The indicator responded different for each model	The indicator does not display similar responses to the various fishing strategies	↓
OH	It was the most sensitive indicators. Although the shape was different between the models, it presented coherent direction	The direction of the response was coherent between the scenarios, unlike the shape of the curves	↓
A/DC	The indicator was sensitive to the models	The direction of the responses was not clear, except for OSMOSE that resulted in increase of the indicator in all fishing strategies	↓
R/DC	The indicator was sensitive to the models	The indicator does not display similar responses to the fishing mortality across fishing strategies	↓
APL	The indicator was sensitive to the models	The indicator does not display similar responses to fishing mortality across fishing strategies	↓
C	The indicator was sensitive to the models	The direction of the responses was not clear, except for OSMOSE that resulted in decrease of the indicator in all fishing strategies	↓

Moreover, the specificity and sensitivity to the models and ecosystems requires the use of a set of network indicators instead of selecting a single one. The set of indicators are pillars to ensure a robust interpretation of the ecosystem responses to stress. Finally, further work should be carried out to investigate multiple stressors to understand synergism and antagonism, for instance changes in primary production that could

buffer the effects of fishing pressure on the indicators (Shin et al., 2018).

4. Conclusions

In this study, the use of two different models was essential for understanding the behavior of indicators in response to fishing pressure. The comparison of the models allowed us to question the indicators sensitivity and adapt the trophic interactions networks (i.e. modified Atlantis). Such a comparison was essential to understand the mechanisms that modulated the responses of the networks built from the model simulation outputs. Therefore, using different models for computing indicators is useful to strengthen final interpretations on the effects of stressors on the ecosystems. The assumptions of the models differ and we can benefit of the comparison between them to attain robust conclusions on the consequences that fisheries have on the resilience of the ecosystem.

The application of multi-model scenarios simulation confirms the knowledge generated from previous studies (e.g. the Indiseas project) on the specificity of the indicators to the ecosystem models (Shin et al., 2018; Fu et al., 2019). For instance, our results showed that network indicators response to fishing can be influenced by model assumptions as detected by Shin et al. (2018) and the thresholds of the indicators were attained before F would equal the F_{MSY} (Fu et al., 2019). Our study complements the findings of the Indiseas project by testing ecological indicators that consider the complexity of the food web. These indicators are able to detect direct and indirect impacts of fishing pressure on the whole ecosystem, i.e. including benthic, pelagic and non-living compartments. Thus, they are relevant for indicating the status of the ecosystem since they detected changes in ecosystem functioning (de Jonge and Schückel, 2021). The holistic characteristic of the network-indicators made them candidates to integrated ecosystem assessment (McQuatters-Gollop et al., 2022).

In summary, the indicators demonstrated that increasing fishing mortality jeopardizes the ability of the food web to mobilize energy. The decrease of flow evenness that resulted from increasing fishing pressure led to lower diversity and redundancy of trophic interactions, which are essential for the resilience of food webs. Indeed, overfishing endangers ecosystem resilience (Maureaud et al., 2017) and this is problematic mainly due to the challenges imposed by climate change on marine ecosystems (Möllmann et al., 2021). Therefore, proper management of fisheries is needed to guarantee the sustainability of the stocks (Froese et al., 2022). Network indicators are useful to demonstrate dynamics of whole food webs and the interest in using them for management purposes has been increasing (Tam et al., 2017; Safi et al., 2019; Fath et al., 2019). This work was a good exercise to investigate the indicators and we found some coherence in the responses that transcended the fishing strategies and models.

CRediT authorship contribution statement

Maysa Ito: Conceptualization, Data curation, Formal analysis, Investigation, Methodology, Validation, Visualization, Writing – original draft, Writing – review & editing. **Ghassen Halouani:** Conceptualization, Data curation, Formal analysis, Methodology, Validation, Writing – review & editing. **Pierre Cresson:** Conceptualization, Funding acquisition, Methodology, Writing – review & editing. **Carolina Giraldito:** Conceptualization, Methodology, Writing – review & editing. **Raphaël Girardin:** Conceptualization, Data curation, Formal analysis, Funding acquisition, Methodology, Validation, Writing – review & editing.

Declaration of Competing Interest

The authors declare that they have no known competing financial interests or personal relationships that could have appeared to influence the work reported in this paper.

Data availability

Data will be made available on request.

Acknowledgements

This work was financially supported by the European Union (FEDER), the French State, the French Region Hauts-de-France and Ifremer, in the framework of the project CPER MARCO 2015-2021. We would like to thank two reviewers for their constructive and helpful comments on the previous version of this manuscript.

Appendix A. Supplementary data

Supplementary data to this article can be found online at <https://doi.org/10.1016/j.ecolind.2023.110011>.

References

- Abarca-Arenas, L.G., Ulanowicz, R.E., 2002. The effects of taxonomic aggregation on network analysis. *Ecol. Model.* 149 (3), 285–296. [https://doi.org/10.1016/S0304-3800\(01\)00474-4](https://doi.org/10.1016/S0304-3800(01)00474-4).
- Allesina, S., Bondavalli, C., 2003. Steady state of ecosystem flow networks: a comparison between balancing procedures. *Ecol. Model.* 165 (2–3), 221–229. [https://doi.org/10.1016/S0304-3800\(03\)00075-9](https://doi.org/10.1016/S0304-3800(03)00075-9).
- Allesina, S., Bondavalli, C., Scharler, U.M., 2005. The consequences of the aggregation of detritus pools in ecological networks. *Ecol. Model.* 189 (1–2), 221–232. <https://doi.org/10.1016/j.ecolmodel.2005.04.002>.
- Audzijonyte, A., Pethybridge, H., Porobic, J., Gorton, R., Kaplan, I., Fulton, E.A., 2019. AtlAntis: A spatially explicit end-to-end marine ecosystem model with dynamically integrated physics, ecology and socio-economic modules. *Methods Ecol. Evol.* 10 (10), 1814–1819. <https://doi.org/10.1111/2041-210X.13272>.
- Borer, E.T., Halpern, B.S., Seabloom, E.W., 2006. Asymmetry in community regulation: effects of predators and productivity. *Ecology* 87 (11), 2813–2820. [https://doi.org/10.1890/0012-9658\(2006\)87\[2813:AICREO\]2.0.CO;2](https://doi.org/10.1890/0012-9658(2006)87[2813:AICREO]2.0.CO;2).
- Borrett, S.R., Lau, M.K., 2014. enaR: an R package for ecosystem network analysis. *Methods Ecol. Evol.* 5 (11), 1206–1213. <https://doi.org/10.1111/2041-210X.12282>.
- Bracis, C., Lehuta, S., Savina-Rolland, M., Travers-Trolet, M., Girardin, R., 2020. Improving confidence in complex ecosystem models: the sensitivity analysis of an Atlantis ecosystem model. *Ecol. Model.* 431, 109133 <https://doi.org/10.1016/j.ecolmodel.2020.109133>.
- Briton, F., Shannon, L., Barrier, N., Verley, P., Shin, Y.J., 2019. Reference levels of ecosystem indicators at multispecies maximum sustainable yield. *ICES J. Mar. Sci.* 76 (7), 2070–2081. <https://doi.org/10.1093/icesjms/fsz104>.
- Coll, M., Shannon, L.J., Kleisner, K.M., Juan-Jordá, M.J., Bundy, A., Akoglu, A.G., Banaru, D., Boldt, J.L., Borges, M.F., Cook, A., Diallo, I., 2016. Ecological indicators to capture the effects of fishing on biodiversity and conservation status of marine ecosystems. *Ecol. Ind.* 60, 947–962. <https://doi.org/10.1016/j.ecolind.2015.08.048>.
- Cresson, P., Chouvelon, T., Bustamante, P., Bănarau, D., Baudrier, J., Le Loc'h, F., Maufrert, A., Miale, B., Spitz, J., Wessel, N., Briand, M.J., 2020. Primary production and depth drive different trophic structure and functioning of fish assemblages in French marine ecosystems. *Prog. Oceanogr.* 186, 102343 <https://doi.org/10.1016/j.pocean.2020.102343>.
- de Jonge, V.N., Schückel, U., 2021. A comprehensible short list of ecological network analysis indices to boost real ecosystem-based management and policy making. *Ocean Coast. Manag.* 208, 105582 <https://doi.org/10.1016/j.ocecoaman.2021.105582>.
- de la Vega, C., Schückel, U., Horn, S., Kröncke, I., Asmus, R., Asmus, H., 2018. How to include ecological network analysis results in management? A case study of three tidal basins of the Wadden Sea, south-eastern North Sea. *Ocean Coast. Manag.* 163, 401–416. <https://doi.org/10.1016/j.ocecoaman.2018.07.019>.
- Fath, B.D., Scharler, U.M., Ulanowicz, R.E., Hannon, B., 2007. Ecological network analysis: network construction. *Ecol. Model.* 208 (1), 49–55. <https://doi.org/10.1016/j.ecolmodel.2007.04.029>.
- Fath, B.D., Asmus, H., Asmus, R., Baird, D., Borrett, S.R., de Jonge, V.N., Ludovisi, A., Niquil, N., Scharler, U.M., Schückel, U., Wolff, M., 2019. Ecological network analysis metrics: the need for an entire ecosystem approach in management and policy. *Ocean Coast. Manag.* 174, 1–14. <https://doi.org/10.1016/j.ocecoaman.2019.03.007>.
- Finn, J.T., 1976. Measures of ecosystem structure and function derived from analysis of flows. *J. Theor. Biol.* 56 (2), 363–380. [https://doi.org/10.1016/S0022-5193\(76\)80080-X](https://doi.org/10.1016/S0022-5193(76)80080-X).
- Froese, R. & Pauly, D. *FishBase* <<http://www.fishbase.org>> (2021).
- Froese, R., Papaioannou, E., Scotti, M., 2022. Climate change or mismanagement? *Environ. Biol. Fishes* 1–18. <https://doi.org/10.1007/s10641-021-01209-1>.
- Fu, C., Travers-Trolet, M., Velez, L., Grüss, A., Bundy, A., Shannon, L.J., Fulton, E.A., Akoglu, E., Houle, J.E., Coll, M., Verley, P., 2018. Risky business: the combined effects of fishing and changes in primary productivity on fish communities. *Ecol. Model.* 368, 265–276. <https://doi.org/10.1016/j.ecolmodel.2017.12.003>.

- Fu, C., Xu, Y., Bundy, A., Grüss, A., Coll, M., Heymans, J.J., Fulton, E.A., Shannon, L., Halouani, G., Velez, L., Akoglu, E., 2019. Making ecological indicators management ready: assessing the specificity, sensitivity, and threshold response of ecological indicators. *Ecol. Ind.* 105, 16–28. <https://doi.org/10.1016/j.ecolind.2019.05.055>.
- Fu, C., Xu, Y., Grüss, A., Bundy, A., Shannon, L., Heymans, J.J., Halouani, G., Akoglu, E., Lynam, C.P., Coll, M., Fulton, E.A., 2020. Responses of ecological indicators to fishing pressure under environmental change: exploring non-linearity and thresholds. *ICES J. Mar. Sci.* 77 (4), 1516–1531. <https://doi.org/10.1093/icesjms/fsz182>.
- Fulton, E.A., Parslow, J.S., Smith, A.D., Johnson, C.R., 2004. Biogeochemical marine ecosystem models II: the effect of physiological detail on model performance. *Ecol. Model.* 173 (4), 371–406. <https://doi.org/10.1016/j.ecolmodel.2003.09.024>.
- Fulton, E.A., Smith, A.D., Punt, A.E., 2005. Which ecological indicators can robustly detect effects of fishing? *ICES J. Mar. Sci.* 62 (3), 540–551. <https://doi.org/10.1016/j.icesjms.2004.12.012>.
- Fulton, E.A., Link, J.S., Kaplan, I.C., Savina-Rolland, M., Johnson, P., Ainsworth, C., Horne, P., Gorton, R., Gamble, R.J., Smith, A.D., Smith, D.C., 2011. Lessons in modelling and management of marine ecosystems: the Atlantis experience. *Fish Fish.* 12 (2), 171–188. <https://doi.org/10.1111/j.1467-2979.2011.00412.x>.
- Funes, M., Saravia, L.A., Cordone, G., Iribarne, O.O., Galván, D.E., 2022. Network analysis suggests changes in food web stability produced by bottom trawl fishery in Patagonia. *Sci. Rep.* 12 (1), 1–10. <https://doi.org/10.1038/s41598-022-14363-y>.
- García, S.M., Cochrane, K.L., 2005. Ecosystem approach to fisheries: a review of implementation guidelines. *ICES J. Mar. Sci.* 62 (3), 311–318. <https://doi.org/10.1016/j.icesjms.2004.12.003>.
- Giraldo, C., Ernande, B., Cresson, P., Kopp, D., Cachera, M., Travers-Trolet, M., Lefebvre, S., 2017. Depth gradient in the resource use of a fish community from a semi-enclosed sea. *Limnol. Oceanogr.* 62 (5), 2213–2226. <https://doi.org/10.1002/lno.10561>.
- Girardin, R., Fulton, E.A., Lehuta, S., Rolland, M., Thébaud, O., Travers-Trolet, M., Vermard, Y., Marchal, P., 2018. Identification of the main processes underlying ecosystem functioning in the Eastern English Channel, with a focus on flatfish species, as revealed through the application of the Atlantis end-to-end model. *Estuar. Coast. Shelf Sci.* 201, 208–222. <https://doi.org/10.1016/j.ecss.2016.10.016>.
- Halouani, G., Le Loc'h, F., Shin, Y.J., Velez, L., Hattab, T., Romdhane, M.S., Lasram, F.B.R., 2019. An end-to-end model to evaluate the sensitivity of ecosystem indicators to track fishing impacts. *Ecol. Ind.* 98, 121–130. <https://doi.org/10.1016/j.ecolind.2018.10.061>.
- Halpern, B.S., Walbridge, S., Selkoe, K.A., Kappel, C.V., Micheli, F., d'Agrosa, C., Bruno, J.F., Casey, K.S., Ebert, C., Fox, H.E., Fujita, R., 2008. A global map of human impact on marine ecosystems. *Science* 319 (5865), 948–952. <https://doi.org/10.1126/science.1149345>.
- Hirata, H., Ulanowicz, R.E., 1984. Information theoretical analysis of ecological networks. *Int. J. Syst. Sci.* 15 (3), 261–270. <https://doi.org/10.1080/00207728408926559>.
- Ingeman, K.E., Samhuri, J.F., Stier, A.C., 2019. Ocean recoveries for tomorrow's Earth: Hitting a moving target. *Science* 363 (6425), p.eav1004. <https://doi.org/10.1126/science.aav1004>.
- Johnson, G.A., Niquil, N., Asmus, H., Bacher, C., Asmus, R., Baird, D., 2009. The effects of aggregation on the performance of the inverse method and indicators of network analysis. *Ecol. Model.* 220 (23), 3448–3464. <https://doi.org/10.1016/j.ecolmodel.2009.08.003>.
- Kopp, D., Lefebvre, S., Cachera, M., Villanueva, M.C., Ernande, B., 2015. Reorganization of a marine trophic network along an inshore-offshore gradient due to stronger pelagic-benthic coupling in coastal areas. *Prog. Oceanogr.* 130, 157–171. <https://doi.org/10.1016/j.pocean.2014.11.001>.
- Le Goff, C., Lavaud, R., Cugier, P., Jean, F., Flye-Sainte-Marie, J., Foucher, E., Desroy, N., Fifas, S., Foveau, A., 2017. A coupled biophysical model for the distribution of the great scallop *Pecten maximus* in the English Channel. *J. Mar. Syst.* 167, 55–67. <https://doi.org/10.1016/j.jmarsys.2016.10.013>.
- Lewis, K.A., Rose, K.A., De Mutsert, K., Sable, S., Ainsworth, C., Brady, D.C., Townsend, H., 2021. Using Multiple Ecological Models to Inform Environmental Decision-Making. *Front. Mar. Sci.* 8, 283. <https://doi.org/10.3389/fmars.2021.625790>.
- Magurran, A.E., 2016. How ecosystems change. *Science* 351 (6272), 448–449. <https://doi.org/10.1126/science.aad6758>.
- Marchal, P., Vermard, Y., 2022. Species targeting and discarding in mixed fisheries. *ICES J. Mar. Sci.* <https://doi.org/10.1093/icesjms/fsac095>.
- Martinez, N.D., 1991. Artifacts or attributes? Effects of resolution on the Little Rock Lake food web. *Ecol. Monogr.* 61 (4), 367–392. <https://doi.org/10.2307/2937047>.
- Maureaud, A., Gascuel, D., Colléter, M., Palomares, M.L., Du Pontavice, H., Pauly, D., Cheung, W.W., 2017. Global change in the trophic functioning of marine food webs. *PLoS One* 12 (8), e0182826.
- McQuatters-Gollop, A., Guerin, L., Arroyo, N.L., Aubert, A., Artigas, L.F., Bedford, J., Corcoran, E., Dierschke, V., Elliott, S.A.M., Geelhoed, S.C.V., Gilles, A., 2022. Assessing the state of marine biodiversity in the Northeast Atlantic. *Ecol. Ind.* 141, 109148. <https://doi.org/10.1016/j.ecolind.2022.109148>.
- Metcalfe, K., Vaz, S., Engelhard, G.H., Villanueva, M.C., Smith, R.J., Mackinson, S., 2015. Evaluating conservation and fisheries management strategies by linking spatial prioritization software and ecosystem and fisheries modelling tools. *J. Appl. Ecol.* 52 (3), 665–674. <https://doi.org/10.1111/1365-2664.12404>.
- Möllmann, C., Cormon, X., Funk, S., Otto, S.A., Schmidt, J.O., Schwermer, H., Sguotti, C., Voss, R., Quaa, M., 2021. Tipping point realized in cod fishery. *Sci. Rep.* 11 (1), 1–12. <https://doi.org/10.1038/s41598-021-93843-z>.
- Mukherjee, J., Scharler, U.M., Fath, B.D., Ray, S., 2015. Measuring sensitivity of robustness and network indices for an estuarine food web model under perturbations. *Ecol. Model.* 306, 160–173. <https://doi.org/10.1016/j.ecolmodel.2014.10.027>.
- Niquil, N., Chaumillon, E., Johnson, G.A., Bertin, X., Grami, B., David, V., Bacher, C., Asmus, H., Baird, D., Asmus, R., 2012. The effect of physical drivers on ecosystem indices derived from ecological network analysis: Comparison across estuarine ecosystems. *Estuar. Coast. Shelf Sci.* 108, 132–143. <https://doi.org/10.1016/j.ecss.2011.12.031>.
- Pauly, D., Christensen, V., Dalsgaard, J., Froese, R., Torres Jr, F., 1998. Fishing down marine food webs. *Science* 279 (5352), 860–863. <https://doi.org/10.1126/science.279.5352.860>.
- Pethybridge, H.R., Fulton, E.A., Hobday, A.J., Blanchard, J., Bulman, C.M., Butler, I.R., Cheung, W.W., Dutra, L.X., Gorton, R., Hutton, T., Mearns, R., 2020. Contrasting futures for Australia's fisheries stocks under IPCC RCP8.5 emissions—a multi-ecosystem model approach. *Front. Marine Sci.* 7, 577964. <https://doi.org/10.3389/fmars.2020.577964>.
- Piatt, J.F., Parrish, J.K., Renner, H.M., Schoen, S.K., Jones, T.T., Arimitsu, M.L., Kuletz, K.J., Bodenstern, B., García-Reyes, M., Duerr, R.S., Corcoran, R.M., 2020. Extreme mortality and reproductive failure of common mures resulting from the northeast Pacific marine heatwave of 2014–2016. *PLoS One* 15 (1), e0226087.
- Plagányi, É.E., Bell, J.D., Bustamante, R.H., Dambacher, J.M., Dennis, D.M., Dichmont, C.M., Dutra, L.X., Fulton, E.A., Hobday, A.J., van Putten, E.I., Smith, F., 2011. Modelling climate-change effects on Australian and Pacific aquatic ecosystems: a review of analytical tools and management implications. *Mar. Freshw. Res.* 62 (9), 1132–1147. <https://doi.org/10.1071/MF10279>.
- R Core Team, 2021. R: A language and environment for statistical computing. R Foundation for Statistical Computing, Vienna, Austria. <https://www.R-project.org/>.
- Rutledge, R.W., Basore, B.L., Mulholland, R.J., 1976. Ecological stability: an information theory viewpoint. *J. Theor. Biol.* 57 (2), 355–371. [https://doi.org/10.1016/0022-5193\(76\)90007-2](https://doi.org/10.1016/0022-5193(76)90007-2).
- Saavedra, S., Rohr, R.P., Fortuna, M.A., Selva, N., Bascompte, J., 2016. Seasonal species interactions minimize the impact of species turnover on the likelihood of community persistence. *Ecology* 97 (4), 865–873. <https://doi.org/10.1890/15-1013.1>.
- Safi, G., Giebels, D., Arroyo, N.L., Heymans, J.J., Preciado, I., Raoux, A., Schückel, U., Tecchio, S., de Jonge, V.N., Niquil, N., 2019. Vitamine ENA: a framework for the development of ecosystem-based indicators for decision makers. *Ocean Coast. Manag.* 174, 116–130. <https://doi.org/10.1016/j.ocecoaman.2019.03.005>.
- Saint-Béat, B., Baird, D., Asmus, R., Bacher, C., Pacella, S.R., Johnson, G.A., David, V., Vézina, A.F., Niquil, N., 2015. Trophic networks: How do theories link ecosystem structure and functioning to stability properties? A review. *Ecol. Ind.* 52, 458–471. <https://doi.org/10.1016/j.ecolind.2014.12.017>.
- Scotti, M., Bondavalli, C., Bodini, A., Allesina, S., 2009. Using trophic hierarchy to understand food web structure. *Oikos* 118 (11), 1695–1702. <https://doi.org/10.1111/j.1600-0706.2009.17073.x>.
- Sergio, F., Newton, I.A.N., Marchesi, L., Pedrini, P., 2006. Ecologically justified charisma: preservation of top predators delivers biodiversity conservation. *J. Appl. Ecol.* 43 (6), 1049–1055. <https://doi.org/10.1111/j.1365-2664.2006.01218.x>.
- Shannon, L., Coll, M., Bundy, A., Gascuel, D., Heymans, J.J., Kleisner, K., Lynam, C.P., Piroddi, C., Tam, J., Travers-Trolet, M., Shin, Y.J., 2014. Trophic level-based indicators to track fishing impacts across marine ecosystems. *Mar. Ecol. Prog. Ser.* 512, 115–140. <https://doi.org/10.3354/meps10821>.
- Shin, Y.J., Cury, P., 2004. Using an individual-based model of fish assemblages to study the response of size spectra to changes in fishing. *Can. J. Fish. Aquat. Sci.* 61 (3), 414–431. <https://doi.org/10.1139/f03-154>.
- Shin, Y.J., Houle, J.E., Akoglu, E., Blanchard, J.L., Bundy, A., Coll, M., Demarcq, H., Fu, C., Fulton, E.A., Heymans, J.J., Salihoğlu, B., 2018. The specificity of marine ecological indicators to fishing in the face of environmental change: a multi-model evaluation. *Ecol. Ind.* 89, 317–326. <https://doi.org/10.1016/j.ecolind.2018.01.010>.
- Shin, Y.J., Shannon, L.J., 2010. Using indicators for evaluating, comparing, and communicating the ecological status of exploited marine ecosystems. 1. The IndiSeas project. *ICES J. Mar. Sci.* 67 (4), 686–691. <https://doi.org/10.1093/icesjms/fsp273>.
- Smith, M.D., Fulton, E.A., Day, R.W., Shannon, L.J., Shin, Y.J., 2015. Ecosystem modelling in the southern Benguela: comparisons of Atlantis, Ecosim, and OSMOSE under fishing scenarios. *Afr. J. Mar. Sci.* 37 (1), 65–78. <https://doi.org/10.2989/1814232X.2015.1013501>.
- Spence, M.A., Blanchard, J.L., Rossberg, A.G., Heath, M.R., Heymans, J.J., Mackinson, S., Serpenti, N., Speirs, D.C., Thorpe, R.B., Blackwell, P.G., 2018. A general framework for combining ecosystem models. *Fish Fish.* 19 (6), 1031–1042. <https://doi.org/10.1111/faf.12310>.
- Tam, J.C., Link, J.S., Rossberg, A.G., Rogers, S.I., Levin, P.S., Rochet, M.J., Bundy, A., Belgrano, A., Libralato, S., Tomczak, M., Van De Wolfshaar, K., 2017. Towards ecosystem-based management: identifying operational food-web indicators for marine ecosystems. *ICES J. Mar. Sci.* 74 (7), 2040–2052. <https://doi.org/10.1093/icesjms/fsw230>.
- Thompson, S.A., Sydemann, W.J., Santora, J.A., Black, B.A., Suryan, R.M., Calambokidis, J., Peterson, W.T., Bograd, S.J., 2012. Linking predators to seasonality of upwelling: using food web indicators and path analysis to infer trophic connections. *Prog. Oceanogr.* 101 (1), 106–120. <https://doi.org/10.1016/j.pocean.2012.02.001>.
- Timmerman, C.A., Marchal, P., Denamiel, M., Couvreur, C., Cresson, P., 2020. Seasonal and ontogenetic variation of whiting diet in the Eastern English Channel and the Southern North Sea. *PLoS One* 15 (9), e0239436.
- Timmerman, C.A., Giraldo, C., Cresson, P., Ernande, B., Travers-Trolet, M., Rouquette, M., Denamiel, M., Lefebvre, S., 2021. Plasticity of trophic interactions in fish assemblages results in temporal stability of benthic-pelagic couplings. *Mar. Environ. Res.* 170, 105412. <https://doi.org/10.1016/j.marenvres.2021.105412>.

- Travers-Trolet, M., Coppin, F., Cresson, P., Cugier, P., Oliveros-Ramos, R., Verley, P., 2019. Emergence of negative trophic level-size relationships from a size-based, individual-based multispecies fish model. *Ecol. Model.* 410, 108800 <https://doi.org/10.1016/j.ecolmodel.2019.108800>.
- Travers-Trolet, M., Bourdaud, P., Genu, M., Velez, L., Vermard, Y., 2020. The risky decrease of fishing reference points under climate change. *Front. Mar. Sci.* 7, 850. <https://doi.org/10.3389/fmars.2020.568232>.
- Ulanowicz, R.E., 2001. Information theory in ecology. *Comput. Chem.* 25 (4), 393–399. [https://doi.org/10.1016/S0097-8485\(01\)00073-0](https://doi.org/10.1016/S0097-8485(01)00073-0).
- Ulanowicz, R.E., 2004. Quantitative methods for ecological network analysis. *Comput. Biol. Chem.* 28 (5–6), 321–339. <https://doi.org/10.1016/j.compbiolchem.2004.09.001>.
- Vasas, V., Lancelot, C., Rousseau, V., Jordán, F., 2007. Eutrophication and overfishing in temperate nearshore pelagic food webs: a network perspective. *Mar. Ecol. Prog. Ser.* 336, 1–14. <https://doi.org/10.3354/meps336001>.
- Wood, S.N., 2017. In: *Generalized Additive Models: An Introduction with R*, 2nd ed. Chapman and Hall/CRC Press, London, UK. <https://doi.org/10.1201/9781315370279>.